

Short-range order in amorphous germanium-nitrogen alloys studied by extended x-ray-absorption fine-structure spectroscopy

F. Boscherini,* A. Filippini, S. Pascarelli, and F. Evangelisti

Dipartimento di Fisica, Università "La Sapienza," Piazzale Aldo Moro 2, I-00185 Roma, Italy

S. Mobilio

Istituto Nazionale di Fisica Nucleare, Laboratori Nazionali di Frascati, Casella Postale 13, I-00044 Frascati (Roma), Italy

F. C. Marques and I. Chambouleyron

Instituto de Física, Universidade Estadual de Campinas (UNICAMP), Caixa Postal 6165, 13 081 Campinas, Brazil

(Received 7 July 1988; revised manuscript received 24 October 1988)

We present a study of local order in the novel semiconductor alloy $a\text{-Ge}_{1-x}\text{N}_x\text{:H}$ using extended x-ray-absorption fine structure (EXAFS) at the Ge K edge. We find that the first coordination shell is composed of Ge and N, the relative importance of which varies with the total N concentration. A careful analysis also allowed us to identify a second-shell contribution due to Ge atoms linked to the central Ge via N. All mean interatomic distances were found to be independent of nitrogen concentration. By measuring the mean-square relative fluctuation of the second-shell interatomic distance we give an upper limit to nitrogen bond-angle fluctuations, providing the first such determination by EXAFS in amorphous semiconductor alloys.

INTRODUCTION

The study of amorphous semiconductors and their alloys has recently attracted much attention because of their intriguing physical properties and variety of applications in microelectronics.¹

Recently, $a\text{-Ge}_{1-x}\text{N}_x\text{:H}$ films have been studied as a function of composition by one of the present authors.² It was found that the optical gap could be continuously varied by changing the N partial pressure in the rf sputtering of a Ge target. The absence of infrared absorption at the frequencies corresponding to Ge—H and Ge—H₂ bonding indicates that H atoms are bonded preferentially to N.³ However, at present there are no structural studies available on this material; also, a comparison with the related $a\text{-Si}_{1-x}\text{N}_x\text{:H}$ system would be interesting.

In fact, $a\text{-Si}_{1-x}\text{N}_x\text{:H}$ thin films have been intensely studied. Electron-diffraction measurements on $a\text{-Si}_{1-x}\text{N}_x\text{:H}$ films obtained by the glow discharge of silane and ammonia mixtures⁴ yielded radial distribution functions (RDF's) for this material. It was found that the peaks in the RDF's are a combination of those expected for the first- and second-nearest neighbors in $c\text{-Si}_3\text{N}_4$ and Si. More structural information was obtained by x-ray diffraction⁵ and neutron scattering⁶ on nearly stoichiometric samples deposited by chemical-vapor deposition (CVD). The RDF of the amorphous phase was found to resemble that of β -phase $c\text{-Si}_3\text{N}_4$ and bond angles of 109.8° and 121° were found around Si and N, respectively. Moreover, analysis of small-angle-scattering results pointed to the existence of voids, the presence of which slightly reduces the coordination numbers of Si and N.

As for the compositional disorder, the authors of the electron-diffraction study⁴ interpreted their measurements within the so-called cluster model in which the material is composed of microscopic islands of $c\text{-Si}_3\text{N}_4$ with an $a\text{-Si}$ interconnecting network. However, analysis of optical spectra⁷ and of Si 2*p* photoemission⁸ shows that this model is incorrect and that a continuous random network (CRN) more closely resembles reality. In this model all bonding configurations, Si—(Si_NN_{4-N}) are possible.

Extended x-ray-absorption fine-structure (EXAFS) spectroscopy is an ideal tool to study local order in amorphous semiconductors and their alloys.⁹⁻¹¹ The possibility, afforded by synchrotron radiation emitted by electron storage rings, of "tuning in" to a particular absorption edge and thus studying local bonding properties (bond distances, coordination numbers, and atomic mean-square relative displacements) around each particular chemical species in a binary alloy is a specific advantage of this technique. Among the amorphous semiconductor systems recently studied are $a\text{-Si}_x\text{Ge}_{1-x}\text{:H}$,¹¹⁻¹³ $a\text{-Si}_x\text{C}_{1-x}\text{:H}$,¹³ and $a\text{-Si}_{1-x}\text{N}_x\text{:H}$.^{11,13} Analysis of those results showed that a common feature in all these binary compounds is the constancy of the average bond lengths as a function of composition. In the case of $a\text{-Si}_{1-x}\text{N}_x\text{:H}$ evidence for a chemical-ordering effect was found.

In the study of amorphous binary alloys it is extremely important to refer to a model system of known stoichiometry (this is particularly true in EXAFS). In our case the obvious choice is crystalline Ge_3N_4 ($c\text{-Ge}_3\text{N}_4$). The structure of this compound is similar to the more widely studied $c\text{-Si}_3\text{N}_4$. Two forms have been identified by x-ray diffraction,¹⁴ and have been named α - and β -phase $c\text{-Si}_3\text{N}_4$, both having a hexagonal crystal lattice. Coordination numbers for Si and N are 4 and 3, re-

spectively. This local structure involves covalent bonds between Si and N in, respectively, tetrahedral and planar configurations,¹⁵ both of which are slightly distorted to accommodate translational symmetry throughout the lattice.

In the following we present a study of local order in $a\text{-Ge}_{1-x}\text{N}_x\text{:H}$ by analysis of Ge K -edge results; structural parameters relative to the first and second coordination shells are obtained and discussed.

EXPERIMENT

The $a\text{-Ge}_{1-x}\text{N}_x\text{:H}$ samples were prepared by radiofrequency (rf) sputtering of a Ge target in a reactive atmosphere in a Leybold-Heraeus Z-400 model system. The base vacuum was 10^{-6} mbar and high-purity gases were used. For one sample (no. 5), N_2 and H_2 were used for the reactive atmosphere, for another only NH_3 , and for the others NH_3 and Ar. The substrate temperature was 180°C and films were deposited on Corning 7059 glass, $c\text{-Si}$ wafers, and aluminum foils (used respectively for optical analysis, infrared measurements, and EXAFS). Sample thickness varied from 0.5 to $3\ \mu\text{m}$ and all samples were amorphous by x-ray inspection. Optical and infrared measurements were performed on Zeiss DMR 21 and JASCO 202 spectrometers, respectively. In some cases it was possible to perform compositional analysis of samples using the electron spectroscopy for chemical analysis (ESCA) technique. Measurements were performed in a VG Scientific surface-analysis chamber using Al $K\alpha$ radiation. In Table I we summarize growth conditions, optical gap, and, when possible, nitrogen concentration of the samples.

EXAFS measurements were performed at the Laboratori Nazionali di Frascati synchrotron-radiation facility, using the emission from the ADONE storage ring during dedicated beam time; the storage ring was operated at 1.5 GeV and the average current was approximately 60 mA. The x-ray radiation was monochromatized using a Si(111) channel-cut crystal.¹⁶ The x-ray absorption was measured by simultaneously recording the current from two

TABLE I. Gases used during the deposition process, values of the optical gap, and, when available, bulk concentration of N for the films investigated.

Sample no.	Gases	Pressure (mbar)	E_g (eV)	x
1	Ar	6×10^{-3}	1.1	0
	NH_3	3×10^{-4}		
2	Ar	8×10^{-3}	1.8	
	NH_3	4×10^{-3}		
3	NH_3	1.2×10^{-2}	2.2	
4	Ar	3×10^{-3}	2.3	0.37
	NH_3	1.6×10^{-2}		
5	N_2	4×10^{-3}	2.1	
	H_2	1×10^{-3}		

ion chambers, one placed upstream and the other downstream from the sample. Samples were held in vacuum and were composed of several layers of thin films deposited on Al foil, so that the total $a\text{-Ge}_{1-x}\text{N}_x\text{:H}$ thickness was approximately $10\ \mu\text{m}$; this thickness was chosen to optimize the signal-to-noise ratio. A $c\text{-Ge}_3\text{N}_4$ sample was also investigated and it consisted in a thin mesh powder supported on polycarbonate membranes.

RESULTS

In the left-hand panel of Fig. 1 we show the x-ray-absorption spectra for the five $a\text{-Ge}_{1-x}\text{N}_x\text{:H}$ samples and for the sample of crystalline $c\text{-Ge}_3\text{N}_4$. The spectra were all taken from the Ge K edge onwards and were at least 1200 eV wide. The spectra shown in Fig. 1 are arbitrarily normalized and the energy scale is correct only for sample no. 1, the others being offset for graphic purposes. EXAFS oscillations are clearly visible in the spectra as modulations of the total absorption coefficient.

The absorption spectra were analyzed according to standard procedures. The preedge region was fitted with a linear function and the absorption above the edge was fitted with a smooth spline curve to simulate the atomic cross section. The difference was normalized by $J\{1 - \frac{2}{3}[(E - E_0)/E_0]\}$, where J is the jump height,¹⁷ to yield normalized EXAFS in k space. E_0 was chosen as the maximum of the first derivative of the absorption edge. The EXAFS oscillations obtained in this way are reported in the right-hand panel of Fig. 1.

Two complementary data analyses were used.¹¹⁻¹³ The Fourier-transform technique provided a qualitative inspection of the general structural features of the materials, while a quantitative determination of the structural parameters was obtained by a thorough analysis in k space.

A. Fourier-transform analysis

The data were multiplied by k and Fourier transformed in the range $k = 3 - 16\ \text{\AA}^{-1}$ with a Hanning window of $0.6\ \text{\AA}^{-1}$. The magnitudes of the Fourier transforms obtained in this way are reported in Fig. 2. Note that the R scale is not corrected for phase shifts and the spectra are reported in the order of increasing N concentration from bottom to top.

As can be seen, the Fourier transform relative to sample no. 1 clearly shows only one peak, corresponding to a Ge—Ge bond distance of $2.45\ \text{\AA}$. This fact is consistent with the finding by ESCA that no N is incorporated in this sample. For elemental amorphous semiconductors, signals originating from higher coordination shells are not observed in the Fourier transforms due to the combination of large σ^2 , the $1/R^2$ term, and the mean-free-path effect. In fact, it has been estimated¹⁸ that the rms fluctuation of the tetrahedral angle must be $\geq 9^\circ$ in order for the second shell to be smeared out in the spectrum.

The spectrum relative to $c\text{-Ge}_3\text{N}_4$ exhibits peaks corresponding to the N first-shell distance, of average value $1.835\ \text{\AA}$, and to the Ge second shell, of average distance $3.18\ \text{\AA}$.¹⁴ Further peaks in the $c\text{-Ge}_3\text{N}_4$ spectrum are due to higher coordination shells.

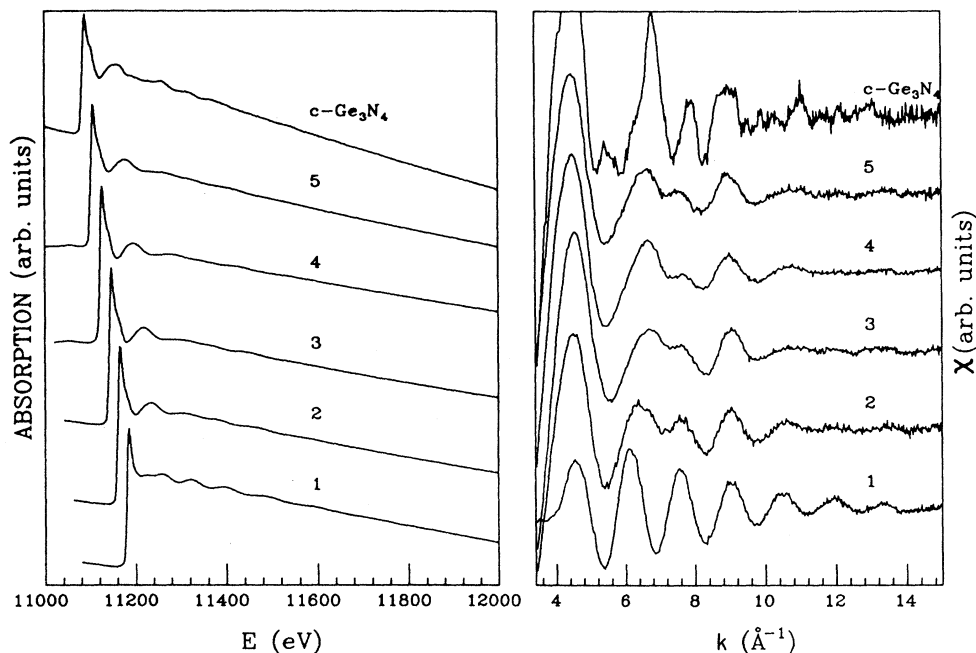


FIG. 1. In the left-hand panel are shown the first 1000 eV of the raw x-ray-absorption data for the $a\text{-Ge}_{1-x}\text{N}_x\text{:H}$ films and for a $c\text{-Ge}_3\text{N}_4$ sample. The energy scale is correct only for sample no. 1, the others being offset for graphic purposes. In the right-hand panel we show the result of background subtraction, that is, the raw EXAFS data.

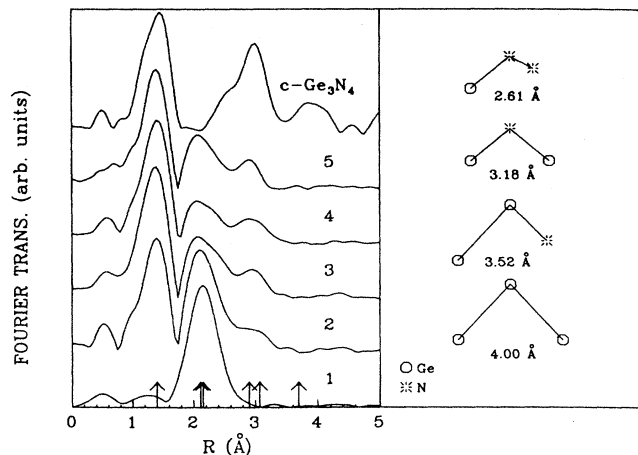


FIG. 2. In the right-hand panel we show the four possible second-shell configurations in $a\text{-Ge}_{1-x}\text{N}_x\text{:H}$ and the interatomic distances expected. Magnitude of the Fourier transforms of EXAFS for the $a\text{-Ge}_{1-x}\text{N}_x\text{:H}$ and $c\text{-Ge}_3\text{N}_4$ samples are shown on the left. The arrows indicate expected positions of features due to possible first- and second-shell configurations, once phase shifts are taken into account. The arrow positions correspond to Ge—N, Ge—Ge, Ge—N—N, Ge—N—Ge, Ge—Ge—N, and Ge—Ge—Ge, respectively, from lower to higher interatomic distances.

The Fourier transforms we obtain for the alloys exhibit peaks in the range from 1 to 3.5 Å. As an aid in identifying the origin of all the peaks, we show as arrows in Fig. 2 the expected positions of signals from all possible first- and second-shell configurations in $a\text{-Ge}_{1-x}\text{N}_x\text{:H}$, when provision is made for the observed phase shifts. Possible second-shell configurations are Ge—N—N, Ge—N—Ge, Ge—Ge—N, and Ge—Ge—Ge, where the first symbol is the central Ge atom and the second and third symbols refer to the atoms in the first and second configuration shells. In calculating the corresponding second-shell distances, we have assumed that all bond lengths are constant and equal to those in the crystalline model compounds, and that Ge and N are, respectively, in tetrahedral and planar configurations; the N—N distance was taken to be 1.15 Å.¹⁹ By inspection of Fig. 2, the first peak is clearly due to a Ge—N pair. The second peak occurs at a position equal to the expected positions for both Ge—Ge and for Ge—N—N; while we certainly expect the Ge—Ge signal to be dominant in the following we shall test for the presence of a Ge—N—N second-shell contribution. The third peak in the Fourier transforms occurs at a position close to that expected for both Ge—N—Ge and Ge—Ge—N. As described in the following, k -space analysis is able to distinguish between these contributions. Clearly, there is no sign of a second-shell Ge—Ge—Ge signal.

B. *k*-space analysis

While Fourier transforms of EXAFS yield an intuitive picture of local coordination, quantitative data analysis is best performed in *k* space. This method is more direct and is generally successfully used when *R*-space analysis is unable to resolve bond distances.¹²

In order to perform this analysis, it is useful to refer to model compounds in which bonding configurations similar to those being investigated are present.¹⁰ In our case the obvious choices are sample no. 1 (*a*-Ge) and *c*-Ge₃N₄, which provide all local structural parameters which enter EXAFS for the Ge—Ge, Ge—N, and Ge—N—Ge configurations. Our analysis procedure for samples with intermediate N concentrations will be to determine all such parameters relative to these models. In this way we determine variations in structural parameters with respect to compounds of known structure; this procedure leads to an improved reliability of results.^{11–13}

As for sample no. 1, it has been established^{9,18,20} that *a*-Ge prepared in different conditions has bond length and coordination number equal to those of *c*-Ge; this has been determined within an error of 1% for the coordination number and of 0.1% for bond lengths.¹⁸ It was also found that the increase in mean-square distribution of bond length ($\Delta\sigma^2$) is equal to $(1.5 \pm 0.15) \times 10^{-3} \text{ \AA}^2$. Results on *a*-Ge:H produced by glow discharge¹² showed

that the same is true for this material, when the incorporation of H in the *a*-Ge network is limited. *a*-Ge, hydrogenated or not, thus constitutes, from the EXAFS point of view, a well-characterized material and we conclude that we are justified in using sample no. 1 as a model for Ge—Ge first-shell bonding.

To illustrate our *k*-space-analysis procedure, we shall describe the procedure on sample no. 4 in detail; results on this sample are representative of all the *a*-Ge_{1-x}N_x:H series. In Fig. 3(a) we compare the experimental EXAFS spectra with the result of backtransforming the *R*-space data to *k* space¹⁰ when the window (in *R* space) was chosen to include all observed features in the spectrum ($R=0.7\text{--}3.6 \text{ \AA}$). Agreement is excellent, and we conclude that by using the Fourier-filtered data we are simply removing noise from the experimental data while retaining the full information corresponding to all coordination shells. In this case, as in all the others we shall describe, the aim is to fit the filtered spectra with linear combinations of model EXAFS signals. The model spectra were obtained as follows. Experimental amplitudes and phases were obtained from scans of sample no. 1 (for Ge—Ge first shell) and from those of *c*-Ge₃N₄ (N first shell and, when required, Ge second shell). These curves were used in the standard EXAFS formula in which provision was made for variation of interatomic distances, of mean-square fluctuations of distances σ^2 , and coordina-

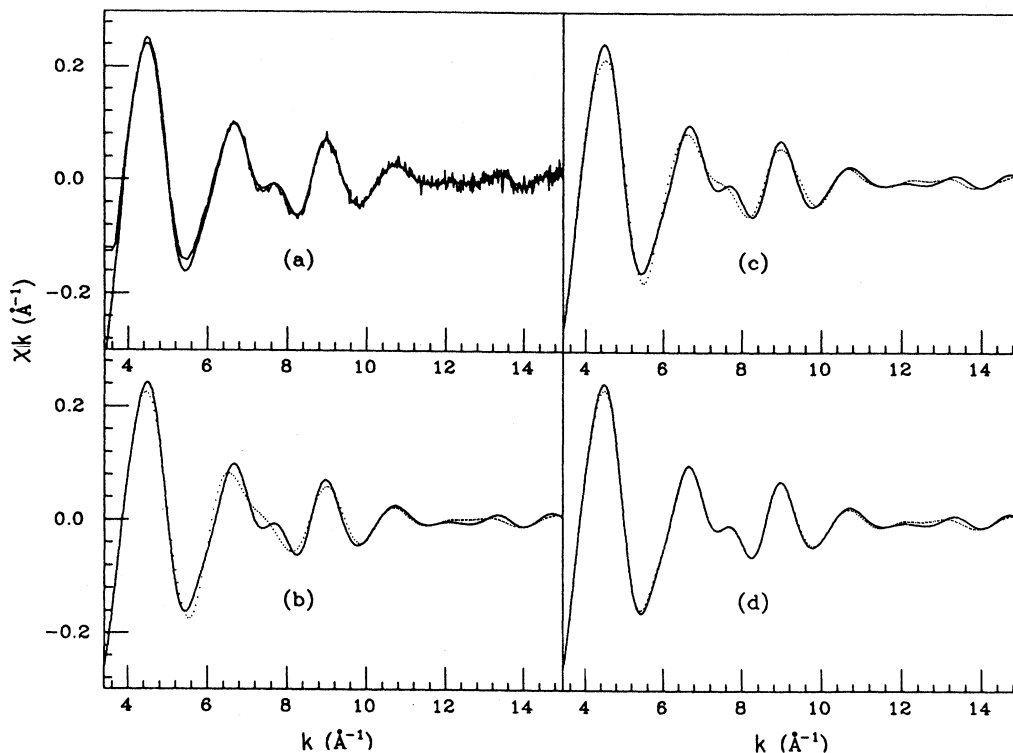


FIG. 3. As an example of the tests performed we show various results relative to sample no. 4. The various panels are explained in detail in the text; best fits to the full EXAFS signal are obtained with the inclusion of a first shell composed of Ge and N and a second shell composed of Ge in a Ge—N—Ge configuration.

TABLE II. Values of the structural parameters obtained from the best fits of the full EXAFS signal. All values are obtained using sample no. 1 and *c*-Ge₃N₄ as models. We have found that for first-shell Ge—Ge $\Delta\sigma^2=0$, relative to sample no. 1.

Sample no.	$N_{\text{Ge-Ge}}$	$R_{\text{Ge-Ge}}$ (Å)	$N_{\text{Ge-N}}$	$R_{\text{Ge-N}}$ (Å)	$\Delta\sigma_{\text{Ge-N}}^2$ (10^{-3} Å ²)	$N_{\text{Ge-N-Ge}}$	$R_{\text{Ge-N-Ge}}$ (Å)	$\Delta\sigma_{\text{Ge-N-Ge}}^2$ (10^{-2} Å ²)
2	1.8	2.44	2.2	1.83	1.9	4.4	3.19	1.1
3	1.4	2.45	2.6	1.81	1.0	5.2	3.19	1.0
4	1.0	2.44	3.0	1.84	2.2	6.0	3.19	1.2
5	1.2	2.43	2.8	1.83	2.7	5.6	3.19	1.2

tion numbers. A linear combination of these individual EXAFS signals was then made and fitted to the Fourier-filtered experimental EXAFS.²¹ For each of the three shells the fitting parameters were the interatomic distance R , the variation of the mean-square distribution of distances $\Delta\sigma^2$, and the coordination number. The best fits were always obtained by fixing the total coordination in the first shell equal to 4.

In Fig. 3(b) we show the fit of the Fourier-filtered EXAFS signal with only a first-shell contribution (Ge—Ge and Ge—N). Clearly, the fit is unsatisfactory, pointing to the presence of extra contributions. In Fig. 3(c) a contribution relative to second-shell N in a Ge—Ge—N configuration was added, but this failed to improve fitting significantly. However, when a Ge contribution relative to second-shell Ge in a Ge—N—Ge configuration was added to the first shell, the fit improved dramatically, as can be seen from Fig. 3(d). Similar behavior was found on all the samples. We have also tested for the presence of Ge—N—N configurations by fitting the result of back-transforming only the first two peaks in the Fourier

transform with either a pure first-shell signal or a first-shell plus a Ge—N—N contribution; we found that inclusion of such a contribution did not lead to significant improvement in the fitting.

We conclude that the full EXAFS signal in *a*-Ge_{1-x}N_x:H can be completely simulated by a first-shell component due to Ge and N and a second shell composed of Ge in a Ge—N—Ge configuration. The relative importance of these contributions varies with N concentration. We can specifically exclude the presence of Ge—N—N, Ge—Ge—N, and Ge—Ge—Ge contributions to EXAFS. While the last two configurations must be present in the material, but are not observed due to the large static angle fluctuations around Ge (see discussion above relative to *a*-Ge), it is justified to conclude that the Ge—N—N configuration is absent; if present, it should appear in the spectra because of the small interatomic distance and, as will be shown in the following, smaller angle fluctuations around N.

We would like to point out that because our fitting procedure is performed in the range $k=3.4-15$ Å⁻¹, we may safely exclude that our result is affected by multiple-scattering effects.²²

A fitting of the type just discussed was applied to all samples and the results are shown in Fig. 4. The values of the fitting parameters obtained in this way are reported in Table II. The determination of the Ge second-shell coordination number presented a problem because the coordination number was found to be highly correlated with $\Delta\sigma^2$; reliable values of these two parameters for the second shell cannot be obtained without further assumptions. By analogy to the *c*-Ge₃N₄ case, we have performed fits by adding the constraint that the number of Ge atoms in the second shell is double the number of N atoms in the first one. This corresponds to the case in which there are no dangling bonds on N or N—H bonds, and, taken as such, is not totally realistic; however, it does yield an upper limit to the value of $\Delta\sigma^2$ for the second shell, a number which is of extreme importance because it is linked to the mean-square fluctuation of the N bond angle.

DISCUSSION

The most obvious feature of the values reported in Table II is the constancy of interatomic distances to within ± 0.015 Å; of all the quantities reported, interatomic distances have the smallest error and greatest reliability. Also, note that the second-shell Ge—Ge distance

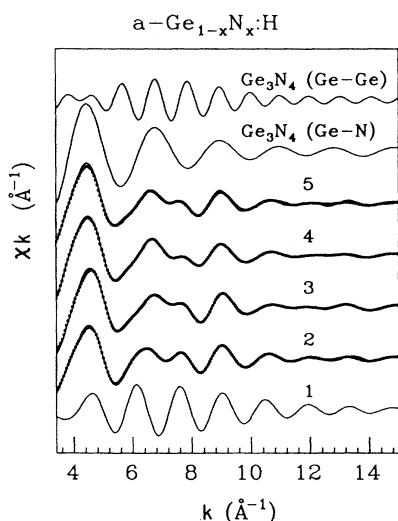


FIG. 4. Best fits to the total EXAFS signal, obtained as explained in the text. We show EXAFS as the solid line and fits as the dotted line; also shown are EXAFS signals from sample no. 1, used as a model for Ge—Ge first-shell EXAFS, and from the Ge—N first shell and the Ge—Ge second shell, the last two obtained from *c*-Ge₃N₄.

is constant and equal to its average value in $c\text{-Ge}_3\text{N}_4$. The constancy of bond lengths has also been observed in other amorphous semiconductor alloys.¹³ The simplest conclusion that can be drawn from the bond-distance values in $a\text{-Ge}_{1-x}\text{N}_x\text{:H}$ is that when N is included in the $a\text{-Ge:H}$ network its bonding to Ge is determined mostly by Ge-N interactions. Notice that the constant value of the Ge-Ge second-shell distance is a further confirmation of this picture. Unfortunately, higher coordination shells cannot be observed, as they might indicate whether the medium-range structure (for example, rings of atoms) is concentration dependent or not; from our first- and second-shell results we would be tempted to infer that it is not; however, further experiments need to be performed with techniques which are more sensitive to medium-range order.

Extreme cases for a network of atoms A and B are a random and a totally chemically ordered network (TCON).²³ In the former type the distribution of atoms is purely statistical and all types of bonds, $A-A$, and $B-B$ are allowed with the same intrinsic probability, while in the latter type $B-B$ bonds are forbidden for A -rich compositions. The fact that we were able to fit the second-shell signal exclusively with Ge in a Ge-N-Ge configuration provides evidence that when N enters the $a\text{-Ge:H}$ network it exclusively forms bonds with Ge atoms and thus forms a TCON. This conclusion is in close agreement with the findings on $a\text{-Si}_{1-x}\text{N}_x\text{:H}$,¹³ where a direct proof of the presence of chemical ordering was obtained from the comparison of the first-shell composition seen by EXAFS with the average atomic composition.

The values we find for $\Delta\sigma^2$ also deserve some comment. The Ge-Ge bond is found to have a mean-square length fluctuation always equal to that found in the $x=0$ limit, while the Ge-N bond has values of $\Delta\sigma^2$ in the range $(1.0-2.7)\times 10^{-3}\text{ \AA}^2$. It is interesting to notice that the lowest value for $\Delta\sigma^2$ is found in sample no. 3, which was deposited without Ar gas in the discharge, the highest value is found in the film deposited with N_2 and H_2 , and similar values are found in the other films deposited under similar conditions. These data might therefore indicate that $\Delta\sigma^2$ is a parameter sensitive to preparation conditions. The values we find for $\Delta\sigma^2$ in the second

shell are always 1 order of magnitude higher than those found in the first shell. This is expected in amorphous semiconductors because of the relatively large bond-angle fluctuations. As discussed above, the values reported in Table II are the maximum values for $\Delta\sigma^2$ because they were obtained under the assumption that the number of second-shell Ge atoms is twice the number of first-shell N atoms. From the value of $\Delta\sigma^2$ obtained this way, we can estimate the root-mean-square bond-angle fluctuations to be $\leq 6^\circ$ in all samples we studied. This value compares well with the minimum fluctuation (9°) found for bond angles on Ge,¹⁸ and implies that bonds on N are more rigid than those on Ge. To our knowledge this is the first determination of bond-angle fluctuations by EXAFS in amorphous semiconductor alloys, and demonstrates that under favorable conditions significant information about coordination shells different from the first can be obtained by EXAFS in disordered systems.

In conclusion, we have performed a study of short-range order in the novel semiconductor alloy $a\text{-Ge}_{1-x}\text{N}_x\text{:H}$. We find that N incorporation in the $a\text{-Ge:H}$ network occurs by formation of a totally chemically ordered network in which first- and second-shell interatomic distances involving Ge were measured to be independent of concentration. Analysis of second-shell EXAFS allowed us to give an upper limit to the Ge-N-Ge bond-angle fluctuation.

ACKNOWLEDGMENTS

One of us (F.B.) would like to acknowledge support by Ente Nazionale Idrocarburi (ENI). This work was supported in part by the Brazilian National Research Council [Conselho Nacional de Desenvolvimento Científico e Tecnológico (CNPq)]. We are indebted to T. Dikonimos Makris, R. Giorgi, and P. Delogu of the Comitato Nazionale per la Ricerca e per lo Sviluppo dell'Energia Nucleare e delle Energie Alternative (ENEA), Centro Ricerche Energetiche della Casaccia for the ESCA measurements. We are grateful to the Laboratori Nazionali di Frascati ADONE machine staff for their collaboration during the experiment and to L. Moretto for skillful technical assistance.

*Present address: Istituto Nazionale di Fisica Nucleare, Laboratori Nazionali di Frascati, Casella Postale 13, 00044 Frascati (Roma), Italy.

¹Proceedings of the 12th International Conference on Amorphous and Liquid Semiconductors, Prague 1987, edited by M. Matyas [J. Non-Cryst. Solids **97&98** (1987)].

²I. Chambouleyron, Appl. Phys. Lett. **47**, 117 (1985).

³I. Chambouleyron, F. Marques, J. Cisneros, F. Alvarez, S. Moehlecke, W. Losch, and I. Pereyra, J. Non-Cryst. Solids **77&78**, 1309 (1985).

⁴M. V. Coleman and D. J. D. Thomas, Phys. Status Solidi **25**, 241 (1968).

⁵T. Aiyama, T. Fukunaga, K. Nihara, T. Hirai, and K. Suzuki, J. Non-Cryst. Solids **33**, 131 (1979).

⁶M. Misawa, T. Fukunaga, K. Nihara, T. Hirai, and K. Suzuki,

J. Non-Cryst. Solids **34**, 313 (1979).

⁷H. Philipp, J. Non-Cryst. Solids **8-10**, 627 (1972).

⁸R. Karcher, L. Ley, and R. L. Johnson, Phys. Rev. **30**, 1896 (1984).

⁹D. Sayers, E. Stern, and F. W. Lytle, Phys. Rev. Lett. **27**, 1204 (1971).

¹⁰P. A. Lee, P. H. Citrin, P. Eisenberger, and B. M. Kincaid, Rev. Mod. Phys. **53**, 769 (1981).

¹¹S. Mobilio and A. Filippini, J. Non-Cryst. Solids **97&98**, 365 (1987).

¹²L. Incoccia, S. Mobilio, M. G. Proietti, P. Fiorini, C. Giovannella, and F. Evangelisti, Phys. Rev. B **31**, 1028 (1985).

¹³A. Filippini, P. Fiorini, F. Evangelisti, and S. Mobilio, MRS Symp. Proc. **95**, 305 (1987).

¹⁴D. Hardie and K. H. Jack, Nature (London) **180**, 332 (1957);

- R. Grun, *Acta Crystallogr. Sect. B* **35**, 800 (1979).
- ¹⁵J. Robertson, *Philos. Mag.* **44**, 215 (1981).
- ¹⁶Laboratori Nazionali di Frascati Internal Report No. 80/79, p. 25 (1980) (unpublished); Laboratori Nazionali di Frascati Internal Report No. 82/51, p. 27 (1982) (unpublished).
- ¹⁷B. Lengeler and P. Eisenberger, *Phys. Rev. B* **21**, 4507 (1980).
- ¹⁸G. Stegemann and B. Lengeler, *J. Phys. (Paris) Colloq.* **47**, C8-407 (1986).
- ¹⁹*CRC Handbook of Chemistry and Physics*, 67th ed. (Chemical Rubber Co., Boca Raton, FL, 1986).
- ²⁰R. J. Temkin, W. Paul, and G. A. N. Connell, *Adv. Phys.* **22**, 581 (1973); D. E. Sayers, E. A. Stern, and F. W. Lytle, *Phys. Rev. Lett.* **27**, 1204 (1971); F. Evangelisti, M. G. Proietti, A. Balzarotti, F. Comin, L. Incoccia, and S. Mobilio, *Solid State Commun.* **37**, 413 (1981); G. Etherington, A. C. Wright, J. T. Wenzel, J. C. Dore, J. H. Clarke, and R. N. Sinclair, *J. Non-Cryst. Solids* **48**, 265 (1982).
- ²¹MINUIT subroutine of the CERN mathematical library.
- ²²M. Benfatto and C. R. Natoli, *J. Phys. (Paris) Colloq.* **47**, C9-1077 (1987).
- ²³S. R. Elliott, *Physics of Amorphous Materials* (Longmans, New York, 1983).